# Absorption spectroscopy of individual nano-objects and improved readout of DNA microarrays using photothermal detection

Stéphane Berciaud, Laurent Cognet, Gerhard Blab, David Lasne, José Remacle, Philippe Tamarat, Brahim Lounis

# Absorption spectroscopy of individual nano-objects and improved readout of DNA microarrays using photothermal detection

Stephane Berciaud,[a] Laurent Cognet [a], Gerhard A. Blab,[a] David Lasne, José Remacle[b], Philippe Tamarat [a] and Brahim Lounis[a]

[a]Centre de Physique Moléculaire Optique et Hertzienne - CNRS UMR 5798 - Université Bordeaux1 351 Cours de la Libération, 33405 Talence, France
[b]Eppendorf Array Technologies, 5000 Namur, Belgium

## ABSTRACT

We developed a photothermal method based on scattering around a nano-absorber that allows for the unprecedented detection of individual nano-objects such as gold nanoparticles with diameter down to 1.4 nm as well as CdSe nanocrystals. This method relies on the absorptive properties of the nano-object and does not suffer from the drawbacks of luminescence-based methods. We present here two different applications of this versatile detection method. First, we performed absorption spectroscopy of individual gold nanoparticles as small as 5*nm* and CdSe nanocrystals in the multiexcitonic regime. Second, we show the applicability of our method for new types of gold nanoparticles based DNA microarrays. In addition to the intrinsic signal stability due to the use of gold labelling, our technique does not require silver staining enhancement and permits to push the signal dynamics of such microarrays from the single nanoparticle detection to almost the full surface coverage.

Keywords: Gold nanoparticles, CdSe nanocrystals, microscopy, absorption spectroscopy, DNA chips.

## INTRODUCTION

In the fast evolving field of nanoscience, where size is crucial for the properties of the objects, simple and sensitive methods for the detection and characterization of single nano-objects are needed. The most commonly used optical techniques are based on luminescence. Single fluorescent molecules have been studied on their own and are now routinely applied in various research domains ranging from quantum optics[1] to life science[2]. In order to study non-luminescent nano-objects, an interesting alternative relies solely on the detection of the absorptive properties. In general, particles with large absorption cross sections and short time intervals between successive absorption events are likely candidates for detection with absorption methods.

Metal nanoparticles (NPs) fulfill both of these requirements: excited near their surface plasmon resonance (SPR) a nanometer sized gold NP has a relatively large absorption cross section ($\sim 10^{-13}$ $cm^2$ for a 5 nm diameter particle) and a fast electron-phonon relaxation time (in the picosecond range)[3]. Since the luminescence yield of these particles is extremely weak, almost all the absorbed energy is converted into heat[4]. The temperature rise induced by the heating leads to a variation of the local index of refraction. Previously, a polarization interference contrast technique has been developed [5] to detect this photothermal effect. The signal consisted in the phase-shift induced between the two spatially-separated beams of an interferometer, when one of the beams propagates through the heated region. Images of gold NPs with diameter of 5*nm* have been recorded with a signal-to-noise ratio SNR ~ 10. But for a given beam intensity, although high, the sensitivity of this technique was ultimately limited by the quality of the overlap of the two arms of the interferometer as well as by their relative phase fluctuations.

We introduced recently a more sensitive and much simpler method called Photothermal Heterodyne Imaging (PHI) for detecting non fluorescent nano-objects[6]. It uses a single probe beam which produces a frequency shifted scattered field as it interacts with time modulated variations of the refraction index around an absorbing nano-object. The scattered field is detected by its beatnote with the probe field which plays the role of a local oscillator as in heterodyne technique.

Because it is not subject to the limitations mentioned above, this allows now for the unprecedented detection of small absorptive objects such as individual metallic clusters composed of 67 atoms and also CdSe/ZnS semiconductor nanocrystals. The PHI method opens new pathways for applications ranging from fundamental physics to neuroscience or biotechnology. In this paper, we begin with an introduction to the principle of this method. We will then focus on two different applications. First PHI can be applied for absorption spectroscopy of small individual NPs. We took advantage of its high sensitivity to study the absorption spectra of individual gold NPs[7] and semiconductor nanocrystals in the multiexcitonic regime[8]. In a fourth section, we show that PHI can be used as a novel readout scheme for gold nanoparticle-based DNA microarrays. It provides direct counting of individual nanoparticles present on each array spot and stable signals, without any silver enhancement. Given the detection of nanometer-sized particles, which minimize the steric hindrance, the linear dynamic range of the method is particularly large and well suited for microarray detection.

## 1. THE PHOTHOTHERMAL HETERODYNE IMAGING METHOD

When an absorbing nano-object embedded in a homogeneous medium is illuminated with an intensity modulated laser beam (modulation frequency $\Omega$)., it behaves like a heat point source. It generates a time-modulated index of refraction in the vicinity of the particle. A probe beam interacting with this profile gives rise to a scattered field containing sidebands with frequency shifts at $\Omega$. As in any heterodyne technique, interference between a reference field (either the reflection of the incident probe at the interface between a cover slip and the sample or its transmission, see Fig. 1(a)) and the scattered field produces a beatnote at the modulation frequency $\Omega$ which can be easily extracted with a lock-in amplifier.

In practice, we overlay a probe beam (633 nm, HeNe laser or 720nm, single frequency Ti:Sa laser) and a heating beam (532 nm, frequency doubled Nd:YAG laser, or tunable cw dye laser (Coherent 599) which intensity is modulated at $\Omega$ = 300 kHz by an acousto-optic modulator (see Fig. 1(a)). The signal is detected in the backward configuration. A combination of a polarizing cube and a quarter wave plate is used to extract the interfering probe-reflected and backward-scattered fields. The intensity of the heating beam ranges from less than $1 MW/cm^2$ to 5 $MW/cm^2$ (depending on the desired signal-to-noise ratio and the nature of the nanoobject to be imaged). Interfering fields are collected on a fast photodiode and fed into a lock-in amplifier in order to extract the beat signal at $\Omega$. Integration times of 10 *ms* are typically used. Images are formed by moving the sample over the fixed laser spots by means of a 2D piezo-scanner. We prepared the samples by spin-coating solutions of nanoobjects diluted in ~1% mass polyvinyl-alcohol (PVA) aqueous solution onto clean microscope coverslips. The dilution and spinning rates were chosen such that the final density of nanoobjects in the samples was less than 1 $\mu m^{-2}$. A drop of viscous silicon oil was added on top of the samples to ensure homogeneity of heat diffusion.

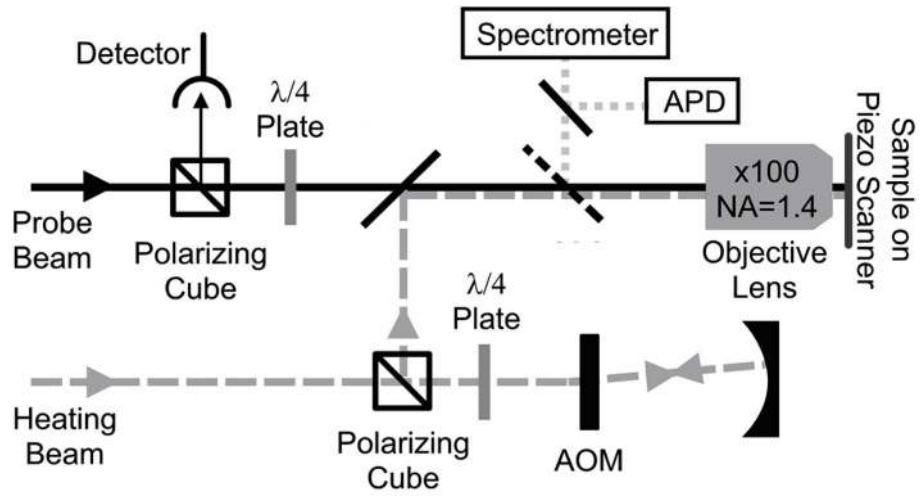


Figure 1. Schematic of the experimental setup for photothermal imaging and absorption spectroscopy. For additional luminescence measurements on semiconductor nanocrystals, a spectrometer and an avalanche photodiode (APD) are used.

## 2. ABSORPTION SPECTROSCOPY OF INDIVIDUAL GOLD NANOPARTICLES

PHI opens new pathways towards absorption spectroscopy of single metallic NP and more generally of non-luminescent nano-objects (see section 3). Several theoretical models predicted the existence of so-called intrinsic size effects in the optical response of metallic NPs with sizes significantly smaller than the electron mean free path[9, 10]. Limitation of the electron mean free path as well as chemical interface damping[9, 11] increase the damping rate of the Surface Plasmon Resonance (SPR), thus leading in the time domain to shorter dephasing times (down to a few fs). Because of such intrinsic size effects, the dielectric constant of the NPs differs from that of the bulk value and must include an additional surface damping contribution. Experimental studies on ensembles of metallic NPs revealed the existence of such effects [9, 12]. However a quantitative description of those effects was made difficult mostly because of inhomogeneous broadening. In order to overcome this shortcoming, PHI was used to record absorption spectra of individual gold NPs with diameters down to 5 *nm*[7]. Figure 2 represents the absorption spectra of 2 single gold NPs with diameters of 33 *nm* and 5 *nm* respectively, performed in the wavelength range 515-580 *nm* (i.e. photon energy range 2.41-2.14 *eV*). The values of peak resonance energies are not particularly affected by intrinsic size effects. On the contrary, a significant increase in width of the resonance that cannot be described by Mie theory using the bulk values of the gold dielectric constant is clearly visible [13]. We found a good agreement between the experimental widths and Mie simulations by introducing the size dependent correction to the bulk dielectric constant that accounts for the presence of intrinsic size effects in the absorption spectra of small gold NPs[7] (Fig. 2 (b)). Although the existence of intrinsic size effects in the optical response of gold NPs was unambiguously revealed, part of the damping processes are due to interband transition, which makes it difficult to connect the widths of the Plasmon resonances to the damping rate. Indeed, for gold, the energy threshold for interband transitions lies at ~2.4 *eV* and is preceded by an absorption tail starting at about 1.8 *eV*. Consequently, the SPR spectra are asymmetric and defining a full-width-at-half maximum of absorption spectra for gold NPs is delicate, and even impossible for very small particles. A way to circumvent this additional damping would consist in red-shifting resonant energies towards photon energy smaller than the onset of interband transition. This can be done either by embedding spherical gold NPs in a matrix with high refractive index or by studying the SPR of the long axis mode in gold nanorods [14, 15] or even by using core-shell NP[16].

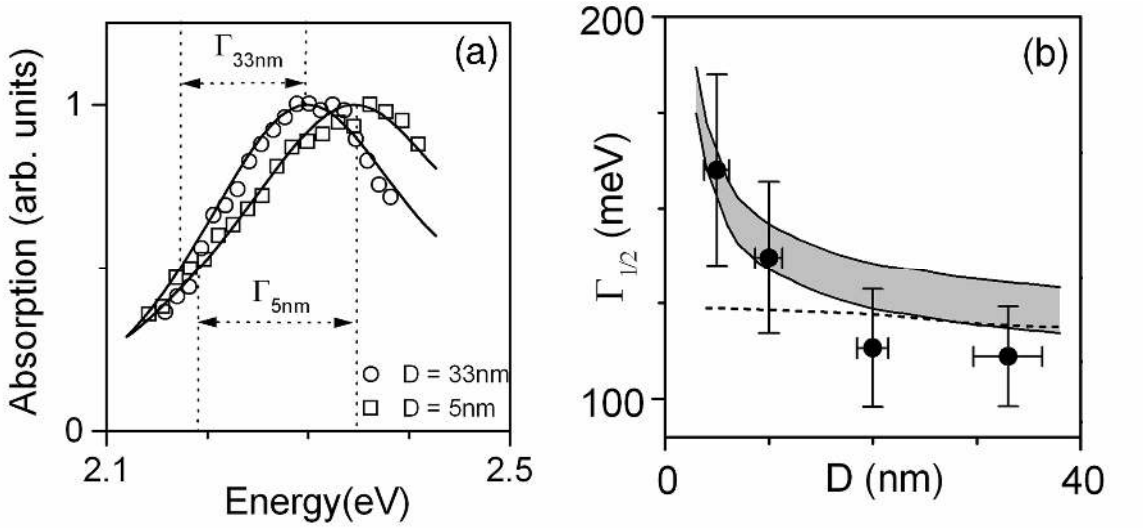


Figure 2. (a) Normalized absorption spectra of 2 single gold NPs of respective diameters equal to 33 *nm* (open circles), and 5 *nm* (open squares).The extracted red width at half maximum $\Gamma_{1/2}$ is shown on both NP spectra. The experimental values are compared with simulations based on Mie theory (solid lines) using size dependant modification in the dielectric constant of gold.
(b) Size dependence of the mean values of the red width at half maximum (circles with standard deviations) are compared with Mie theory using the bulk values of the dielectric constant (dotted line) and a size dependant correction accounting for additional surface damping (gray area) scaling as 1/D. The gray area accounts for the experimental uncertainties on the bulk dielectric function of gold given in [13].

## 3. PHOTOTHERMAL IMAGING AND ABSORPTION SPECTROSCOPY OF INDIVIDUAL SEMICONDUCTOR NANOCRYSTALS IN THE MULTIEXCITONIC REGIME.

PHI can also be used to detect CdSe/ZnS semiconductor nanocrystals. Those nano-objects have relatively high absorption cross-sections[17, 18] (typically ~10-$^{15}$cm²) and when excited with sufficiently high intensities, excitons are created at average rates significantly higher than their radiative recombination rates[17, 19]. In this regime, efficient non-radiative Auger recombinations of the prepared multiexcitons take place[20]. In CdSe/ZnS nanocrystals, these recombinations occur in the picoseconds range as measured in ensemble time resolved experiments[21]. Individual nanocrystals could thus be detected through their absorption using the Photothermal Heterodyne method[6]: Individual fluorescent nanocrystals were first located by recording a 20x20µm² fluorescence image of the sample (Fig.3 (a)). The blinking behavior, a signature of single nanocrystal emission, is clearly visible. We then recorded a photothermal image of the same sample area (Fig.3 (b)). Cleary the luminescence and photothermal images correlate well (>80%) of the luminescence spots correlate with a photothermal spot), proving that the spots in the photothermal image stem from individual nanocrystals. Contrary to luminescence, the photothermal signals do not show any blinking behavior . They remain stable during time scales larger than those necessary to record an absorption spectrum.
Luminescence spectra were recorded in the monoexcitonic regime (with low *cw* excitation intensities). Photothermal absorption spectra were recorded in the high *cw* excitation regime, where excitons are created at average rates significantly higher than the radiative recombination rate of the band edge exciton. In that case, luminescence from monoexcitonic recombination is very weak and the prepared multiexcitons relax rapidly through efficient non-radiative Auger processes. The observed photothermal absorption bands (Fig. 3.c) are assigned to such Auger recombinations involving biexciton and trion states. Comparison with the photoluminescence spectra of the same nanocrystals leads to the measurement of spectral Stokes shifts ΔE free from ensemble averaging. Comparison of the mean value of ΔE with ensemble measurements allows for an estimation of the biexciton and trion binding energies, which are in good agreement with prior theoretical and experimental results[8].

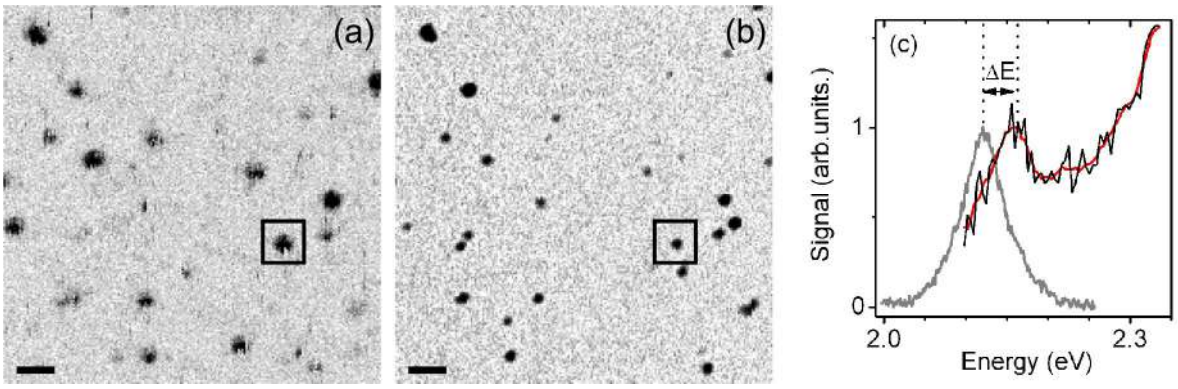

Figure 3. Comparison of photoluminescence (a) and Photothermal Heterodyne images (b) of the same area (20x20 $\mu m^2$) of a sample containing CdSe/ZnS nanocrystals. The integration time per point was 10 ms. Scale bar is 2μm. (c) Photoluminescence (gray line) and photothermal absorption (black line) spectra recorded for a same individual CdSe/ZnS nanocrystal. For clarity a smoothing of the absorption spectra is shown. The homogenous Strokes shift ΔE is also shown.

## 4. OPTICAL READOUT OF GOLD NANOPARTICLE-BASED DNA MICROARRAYS

The determination and exact quantification of gene expression is becoming increasingly important in basic pharmaceutical and clinical research. Fluorescence-based DNA assays are most widely used, but suffer from the presence of autofluorescence in some biological samples and substrates, which severely interferes with the detection of the target molecules. DNA assays based on gold NP (AuNPs) labels present a viable alternative. They commonly use AuNPs larger than 40 nm, which can be readily detected due to their strong light scattering at visible wavelengths[22, 23]. For increased specificity and reactivity, AuNPs smaller than 40 nm are preferred. Indeed, small AuNPs functionalized with oligonucleotides exhibit a very sharp thermal denaturation profile, and the rate of reaction on a surface is much higher than with large particles[24-26]. As small AuNPs (diameter, < 40 nm) barely interact with light, their direct optical detection has been impossible until recently without silver staining enhancement techniques[24, 26]. However, saturation at the amplification step limits the linear dynamic range as the typical size of the silver crystals is much larger than that of the AuNPs[25]. Furthermore, spontaneous conversion of silver solution into metallic grains can occur leading to nonspecific signals[25]. Another alternative is the electrical detection of the AuNPs after catalytic or enzymatic deposition of the silver[27-29]. In this context, the possibility of detecting tiny AuNPs at the single particle level holds great promise for new and more efficient optical readout schemes of DNA assays.

In order to avoid the use of silver enhancement techniques, we used the photothermal method to directly image standard low-density spotted DNA microarrays. These arrays are well suited for routine applications as they contain a limited number of genes (usually below 1000), which enables good spotting quality and good reproducibility[30]. The test arrays were composed of serial dilutions of biotinylated capture probes having a length of 415 bases aminated in their 5' end. The capture probes were synthesized by polymerase chain reaction having one primer aminated at the 5' end. Biotinylated dCTP and dATP were incorporated during the polymerase chain reaction synthesis. Amplicons were purified to remove the excess dNTP and primers, and were spotted on aldehyde-activated slides. Antibiotin/gold (20 nm) conjugates were used (BBInternational, Cardiff, UK). The concentrations corresponded to the full dynamic range afforded by silver staining enhancement imaging.

For each spot of the microarray, we performed images with two different resolutions. In the ''low resolution regime'', 200 x 200 $\mu m^2$ images were acquired with step sizes of 2 μm, i.e. about twice the size of the laser focal spot. In those

conditions, a fast scanning of entire spots is achieved but at the cost of subsampling the surface. In the ‘‘counting regime’’, only a small (central) portion of the spots is scanned (20 x 20 $\mu m^2$ images, 0.2 μm per point). The high resolution of the counting regime ultimately allows for detecting all individual AuNPs. Low resolution images of four different spots are presented in Fig. 4. Regions of total coverage of the surface are found (spots 1–4), in which the outlines of the spots are clearly visible[31]. For those, the average distances between AuNPs are smaller than the scanning resolution that corresponds to a surface density of AuNPs greater than typically one per 1 $\mu m^2$. Our method provides a reliable quantification of the amount of DNA molecules in each spot of the microarrays[32](not shown). This determination is no longer limited by any constraints of the detection method, but only by the degree of unspecific signals on one side and by the size of the AuNPs on the other side. Indeed, as all AuNPs are detected, the lower detection of DNA only depends on unspecific DNA hybridization events and on the quality of surface treatments[31]. Concerning the upper detection limit, the ultimate limit is given by the condition of weak plasmon coupling between particles. Indeed, when the average distance of the AuNPs is comparable to their size, the optical response of AuNPs is modified[33].Furthermore, the possibility to detect much smaller AuNPs (down to 1.4 nm)[6] should significantly increase the dynamic range.

In addition to the high sensitivity and dynamics afforded by the present method, AuNPs-based DNA arrays can be stored for long periods and measured several times. Our approach thus combines the advantages of fluorescence measurements-small marker size, purely optical detection- with the high stability, specificity, and dynamic range afforded by AuNP labelling techniques. This makes photothermal approaches promising for application in biochips.

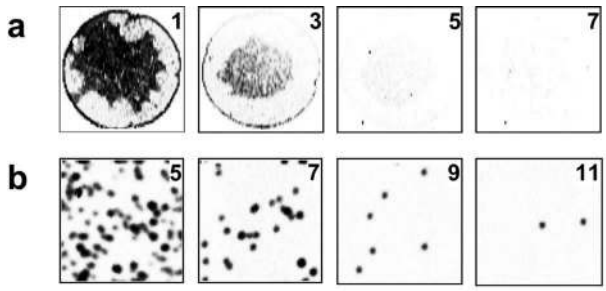


Figure 4. Direct imaging (no silver enhancement) of four spots in the low resolution (a) and counting regime (b).

## CONCLUSION

The present work demonstrates the advantages of photothermal heterodyne detection for absorbing nano-objects. The study of the physical properties of very small metallic aggregates and semiconductor nanocrystals is now possible at the individual object level. We measured for the first time the absorption spectra of individual gold nanoparticules as small as 5 *nm*. We clearly evidenced intrinsic size effects in the optical response of the smallest particles and accessed the homogeneous width of their surface plasmon resonance. The spectroscopy of small gold or silver NP oligomers may also lead to a better understanding of the physical properties of those nanoobjects. This could provide an estimation of the corrections in the photothermal signal that have to be made in concentrated AuNP-based DNA micro assays because of plasmon coupling between close AuNPs. We also demonstrated that our method can be applied to absorption spectroscopy of other nano-objects such as CdSe/ZnS semiconductor nanocrystals in the multiexcitonic regime[8].

## ACKNOWLEDGEMENTS

We thank P. Morin (Coherent France) for the loan of the dye laser. This research was funded by the CNRS and the MENRT (ACI Nanoscience and DRAB) and by Région Aquitaine.

## REFERENCES


1. Lounis, B.; Orrit, M., Single-Photon Sources. *Rep. Prog. Phys.*, 68, 1129 -1179, (2005).
2. Moerner, W. E.; Orrit, M., Illuminating single molecules in condensed matter. *Science*, 283, (5408), 1670-6, (1999).
3. Link, S.; El-Sayed, M. A., Optical properties and ultrafast dynamics of metallic nanocrystals. *Annu Rev Phys Chem*, 54, 331-66, (2003).
4. Berciaud, S.; Lasne, D.; Blab, G. A.; Cognet, L.; Lounis, B., Photothermal Heterodyne Imaging of Individual Metallic Nanoparticles: Theory versus Experiments. *Phys. Rev. B*, In press (2006).
5. Boyer, D.; Tamarat, P.; Maali, A.; Lounis, B.; Orrit, M., Photothermal Imaging of Nanometer-Sized Metal Particles Among Scatterers. *Science*, 297, (5584), 1160-1163, (2002).
6. Berciaud, S.; Cognet, L.; Blab, G. A.; Lounis, B., Photothermal Heterodyne Imaging of Individual Nonfluorescent Nanoclusters and Nanocrystals. *Phys Rev Lett*, 93, (25), 257402, (2004).
7. Berciaud, S.; Cognet, L.; Tamarat, P.; Lounis, B., Observation of Intinsic size effects in the optical response of individual gold nanoparticles. *Nano Letters*, 5, (3), 515-518, (2005).
8. Berciaud, S.; Cognet, L.; Lounis, B., Photothermal absorption spectroscopy of individual semiconductor nanocrystals. *Nano Lett*, 5, (11), 2160-3, (2005).
9. Kreibig, U.; Vollmer, M., *Optical properties of metal clusters*. Springer-Verlag: Berlin, (1995).
10. Link, S.; El Sayed, M. A., Shape and size dependence of radiative, non-radiative and photothermal properties of gold nanocrystals. *Int. Reviews in Physical Chemistry*, 3, (19), 409-453, (2000).
11. Persson, B. N. J., Polarizability of small spherical metal particles: influence of the matrix environment. *Surface Science*, 281, 153-162, (1993).
12. Bosbach, J.; Hendrich, C.; Stietz, F.; Vartanyan, T.; Trager, F., Ultrafast dephasing of surface plasmon excitation in silver nanoparticles: influence of particle size, shape, and chemical surrounding. *Phys Rev Lett*, 89, (25), 257404, (2002).
13. Johnson, P. B.; Christy, R. W., Optical constants of the noble metals. *Phys. Rev. B*, 6, (12), 4370, (1972).
14. Klar, T.; Perner, M.; Grosse, S.; von Plessen, G.; Spirkl, W.; Feldmann, J., Surface-Plasmon Resonances in Single Metallic Nanoparticles. *Phys Rev Lett*, 80, 4249–4252, (1998)
15. Sonnichsen, C.; Franzl, T.; Wilk, T.; von Plessen, G.; Feldmann, J.; Wilson, O.; Mulvaney, P., Drastic reduction of plasmon damping in gold nanorods. *Phys Rev Lett*, 88, (7), 077402, (2002)
16. Prodan, E.; Radloff, C.; Halas, N. J.; Nordlander, P., A hybridization model for the plasmon response of complex nanostructures. *Science*, 302, (5644), 419-22, (2003)
17. Lounis, B.; Bechtel, H. A.; Gerion, D.; Alivisatos, A. P.; Moerner, W. E., Photon antibunching in single CdSe/ZnS quantum dot fluorescence. *Chem.Phys.Lett.*, 329, 399, (2000)
18. Leatherdale, C. A.; Woo, W.-K.; Mikulec, F. V.; Bawendi, M. G., On the absorption cross section of CdSe nanocrystal quantum dots. *J. Phys. Chem. B*, 106, 7619, (2002)
19. Schlegel, G.; Bohnenberger, J.; Potapova, I.; Mews, A., Fluorescence decay time of single semiconductor nanocrystals. *Phys Rev Lett*, 88, (13), 137401, (2002)
20. Efros, A. L.; Lockwood, D. J.; Tsybeskov, L., *Semiconductor Nanocrystals*. Kluwer Academic / Plenum Publishers: New-York, (2003).

21. Klimov, V. I.; Mikhailovsky, A. A.; McBranch, D. W.; Leatherdale, C. A.; Bawendi, M. G., Quantization of multiparticle auger rates in semiconductor quantum dots. *Science*, 287, (5455), 1011-3, (2000).
22. Yguerabide, J.; Yguerabide, E. E., Light-scattering submicroscopic particles as highly fluorescent analogs and their use as tracer labels in clinical and biological applications. *Anal Biochem*, 262, (2), 137-56, (1998).
23. Schultz, S.; Smith, D. R.; Mock, J. J.; Schultz, D. A., Single-target molecule detection with nonbleaching multicolor optical immunolabels. *Proc Natl Acad Sci U S A*, 97, (3), 996-1001, (2000).
24. Taton, T. A.; Mirkin, C. A.; Letsinger, R. L., Scanometric DNA array detection with nanoparticle probes. *Science*, 289, (5485), 1757-60, (2000).
25. Alexandre, I.; Hamels, S.; Dufour, S.; Collet, J.; Zammatteo, N.; De Longueville, F.; Gala, J. L.; Remacle, J., Colorimetric silver detection of DNA microarrays. *Anal Biochem*, 295, (1), 1-8, (2001).
26. Fritzsche, W.; Taton, T. A., Metal nanoparticles as labels for heterogeneous, chip-based DNA detection. *Nanotechnology*, 14, (12), R63-R73, (2003).
27. Park, S. J.; Taton, T. A.; Mirkin, C. A., Array-based electrical detection of DNA with nanoparticle probes. *Science*, 295, (5559), 1503-6, (2002).
28. Möller, R.; Powell, R. D.; Hainfeld, J. F.; Fritzsche, W., Enzymatic Control of Metal Deposition as Key Step for a Low-Background Electrical Detection for DNA Chips. *Nano Letters*, 5, (7), 1475-1482, (2005).
29. Moreno-Hagelsieb, L.; Lobert, P. E.; Pampin, R.; Bourgeois, D.; Remacle, J.; Flandre, D., Sensitive DNA electrical detection based on interdigitated Al/Al2O3 microelectrodes. *Sensors and Actuators B: Chemical*, 98, (2-3), 269-274, (2004).
30. Zammatteo, N.; Hamels, S.; De Longueville, F.; Alexandre, I.; Gala, J. L.; Brasseur, F.; Remacle, J., New chips for molecular biology and diagnostics. *Biotechnol Annu Rev*, 8, 85-101, (2002).
31. Festag, G.; Steinbruck, A.; Wolff, A.; Csaki, A.; Moller, R.; Fritzsche, W., Optimization of gold nanoparticle-based DNA detection for microarrays. *J Fluoresc*, 15, (2), 161-70, (2005).
32. Blab, G. A.; Cognet, L.; Berciaud, S.; Alexandre, I.; Husar, D.; Remacle, J.; Lounis, B., Optical Readout of Gold Nanoparticle-Based DNA Microarrays without Silver Enhancement. *Biophys J*, 90, (1), L13-5, (2006).
33. Sonnichsen, C.; Reinhard, B. M.; Liphardt, J.; Alivisatos, A. P., A molecular ruler based on plasmon coupling of single gold and silver nanoparticles. *Nat Biotechnol*, 23, (6), 741-5, (2005).